Dear Reviewer,

We are very grateful for your comments. We have tried to address each of your concerns and suggestions within the manuscript and outlined our response to your comments below **point-by-point** (our responses are in bold). We think these comments and revisions have strengthened the manuscript and we thank you for your input.

REVIEWER #2

Sharma et al. presented geochemical records for Middle Eocene Climatic Optimum (MECO) from a fluvial sedimentary succession in Spain. The authors attempted to constrain the regional climatic conditions during MECO with a suite of sedimentary archives and geochemical proxies. This is a valuable contribution as few previous studies has identified MECO and assess its climatic implications in terrestrial records. However, the following issues should be addressed/clarified prior to publication.

1) Uncertainties in age constraints

Section 2.2 provided a brief description of the age constraints but discussions about the associated uncertainties in the age models are missing. As the preservation of stratigraphic record is almost always incomplete (e.g. Paola et al., 2018), it is important to provide details on the uncertainties in sample ages and discuss how they affect the interpretation of the geochemical proxies and the comparisons with other records.

We agree that that the fluvial stratigraphic record is particularly incomplete due to the presence of several unconformities during channel formation. However, since the duration of time not preserved cannot be determined and in the absence of other age controls, we rely on a preliminary linear scaling model by correlating the available magnetostratigraphic framework of the Escanilla Formation at Olson to the Geomagnetic Polarity Time Scale (GPTS 2020). This allows us to correlate our geochemical data to the target MECO isotope excursion from ODP site 738. We have tried our best to highlight this in the revised version.

<u>Changes performed in MS:</u>

Line 97 – 109: Added

"The age model used in this study is based on the magnetostratigraphic framework, involving high- and intermediate-quality samples, of the Escanilla Fm by Vinyoles et al., (2020) and agrees well with the magnetostratigraphic interpretation of Bentham et al., (1992). Age constraints by Vinyoles et al., (2020) were also recently used by Peris Cabré

et al., (2023) for the identification of the MECO at Belsue and Yebra de Basa in the Jaca Basin.

To compare our geochemical data relative to the target MECO isotopic excursion from ODP site 738 (Bohaty et al. (2009)) and the Geomagnetic Polarity Time Scale (GPTS 2020) (Ogg 2020), we rely on a preliminary first-order linear scaling by matching the base (at 40 m) and top (at 210 m) of Chron C18n in the magnetostratigraphic data of Vinyoles et al., (2020), to the base of Chron C18n.2n and top of Chron C18n.1n on the Geomagnetic Polarity Time Scale (GPTS 2020) (Figure 1E). All data are presented relative to the thickness of the sampled Olsón section accompanied by the local magnetostratigraphic interpretation of Vinyoles et al., (2020), linearly scaled to the GPTS 2020."

2) Statistical/quantitative analyses

Error bars are missing in many of the plots. Uncertainties estimates were not provided in some of the results. And there's a general lack of statistical analyses for claimed correlation, trend, and changes. See line by line comments for details.

We agree that no error bars or statistical information was provided in the manuscript and have therefore made the necessary changes. This includes describing how uncertainties on data are calculated and reported, including any statistical tests that were performed. We have also modified our figures to represent the standard error. We also want to highlight that in a few instances, standard error can be small relative to the scale at which the data is plotted, giving the impression that error bars have not been plotted.

<u>Changes performed in MS:</u>

Line 214 – 218: Added

"3.9 Uncertainty on reported data

All data reported in this study is associated with uncertainties in the form of standard error of the mean (SE) calculated as $SE = \frac{SD}{\sqrt{n}}$, where SD is the standard deviation and n is the number of replicates analyzed. Uncertainty propagation was done using the uncertainites package on Python (Spyder 4.0.1), which is an open-source and cross-platform program that handles calculations with numbers involving uncertainties."

Line 309 – 315: Added

"The degree of alteration was assessed through the relationship between $\delta^{13}C_{org}$ and $\delta^{13}C_{carb}$, and between $\delta^{18}O_{carb}$ and $\delta^{13}C_{carb}$ values. Pearson correlation coefficient, $r < 0.6$, indicates a statistically non-significant relationship and indicates that a diagenetic overprint on the primary signal can be excluded (e.g., Fio et al., 2010). In both correlation

plots (Figure 6), no statistically significant correlation was found ($\delta^{13}C_{carb}$ vs $\delta^{13}C_{org}$: r = 0.21 (P = .16, N = 45), $\delta^{13}C_{carb}$ vs $\delta^{18}O_{carb}$: r = 0.05 (P = .74, N = 45)) indicating almost none or very minor diagenetic modification of the primary signal. Also, no correlation trend was observed between TOC and $\delta^{13}C_{org}$ (supplementary material; Figure S1)."

Line 239: Modified Figure 3

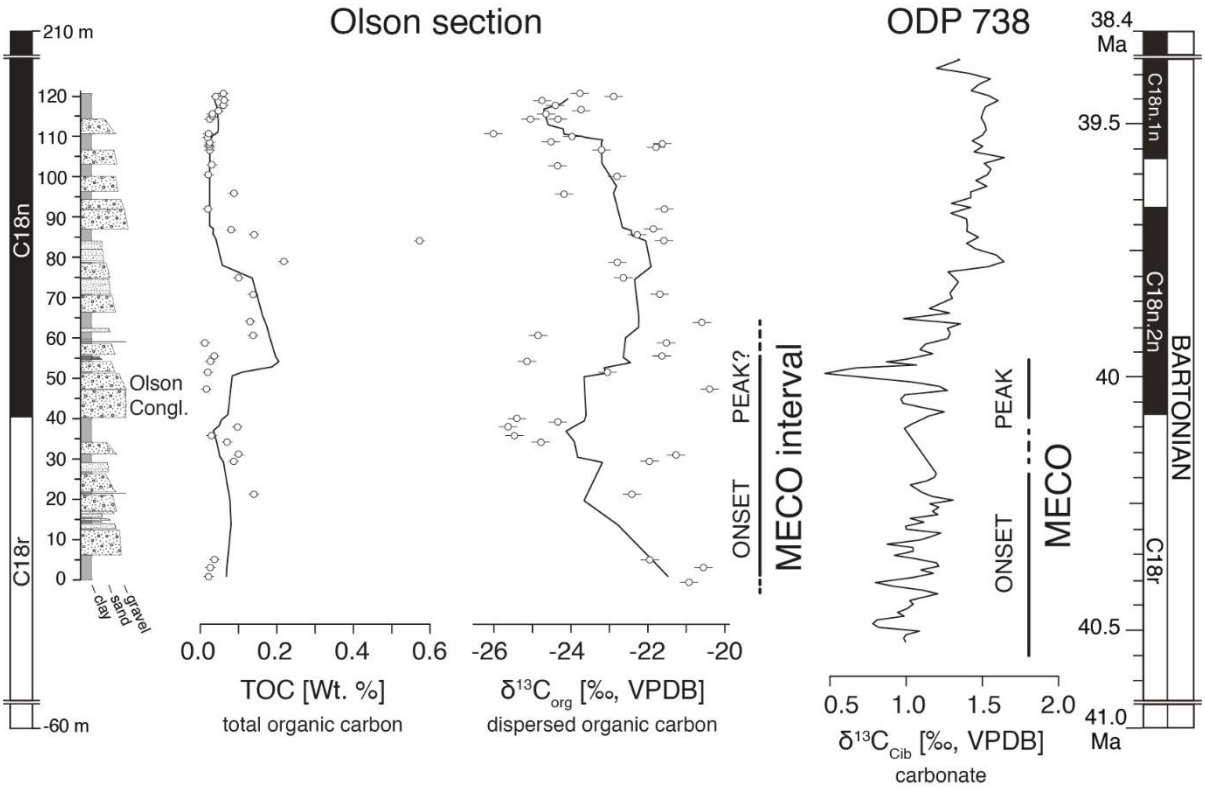

Line 238 – 240: Modified caption of Figure 3.

"Figure 3. Total organic carbon (TOC) and dispersed organic carbon isotope compositions ($\delta^{13}C_{org}$), and associated standard error, in paleosol samples (white circles) presented with a 7-point moving average. Also displayed is the change in benthic foraminiferal (genus *Cibicidoides*) carbon isotope ratios ($\delta^{13}C_{Cib}$) from ODP site 738."

Line 278: Modified Figure 4

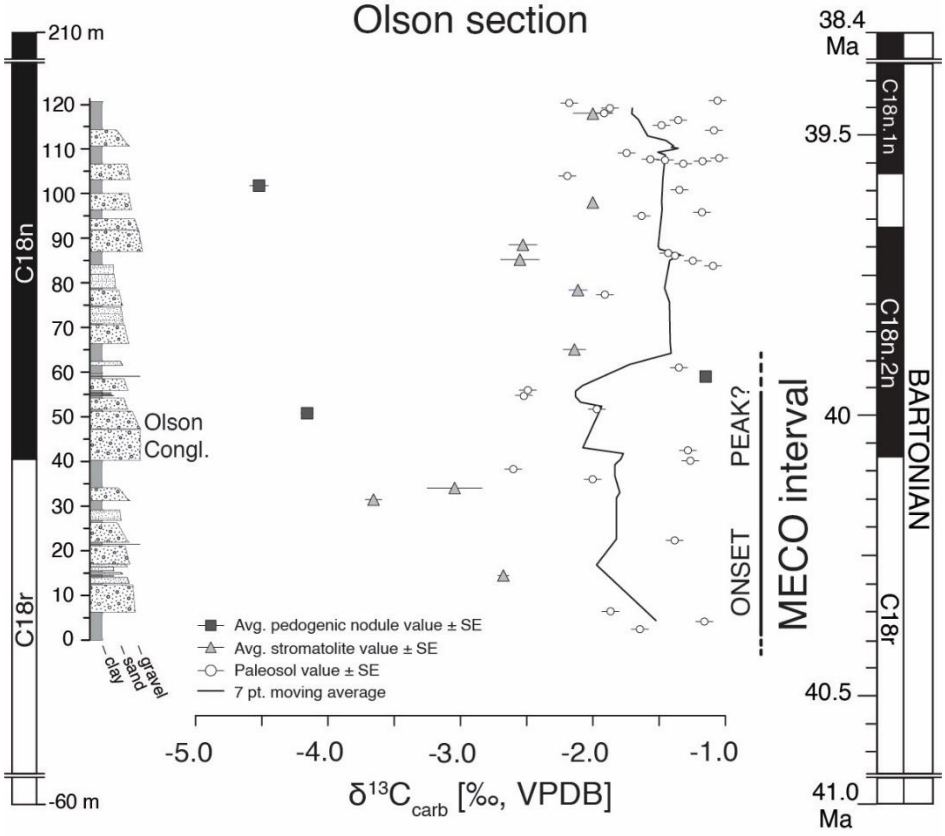

Line 279 – 281: Modified caption of Figure 4.

"Figure 4. Carbon isotope compositions ($\delta^{13}C_{carb}$) and associated standard error from paleosol bulk carbonates (white circles) with a 7-point moving average, and from stromatolite (triangles) and pedogenic nodules (squares) for the Olsón section. Also marked is the MECO onset and peak interval based on $\delta^{13}C_{org}$ values from this study."

Line 292: Modified Figure 5

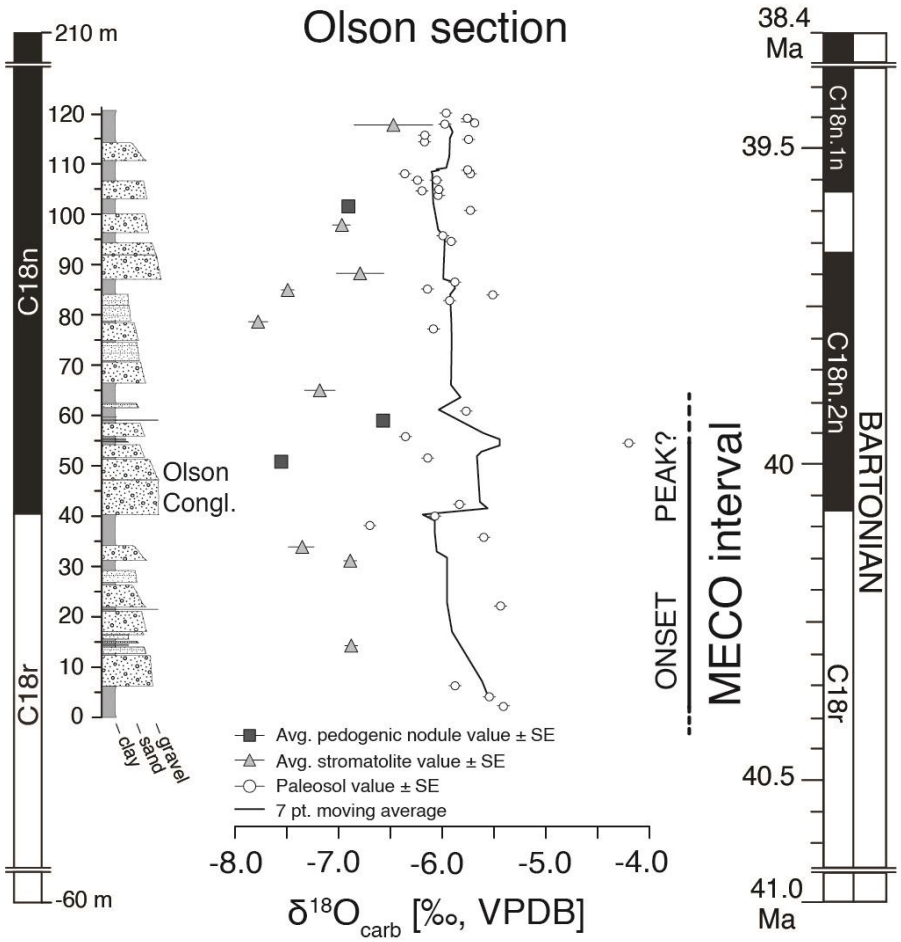

Line 293 – 295: Modified caption of Figure 5

"Figure 5. Oxygen isotope compositions ($\delta^{18}O_{carb}$) from paleosol bulk carbonates (white circles) with a 7-point moving average and associated standard error, and carbonate samples (stromatolites (triangles) and pedogenic nodules (squares)) for the Olsón section. Also marked is the MECO onset and peak interval based on $\delta^{13}C_{org}$ values from this study."

Line 348 – 350: Modified Figure 7 and caption of Figure 7

“

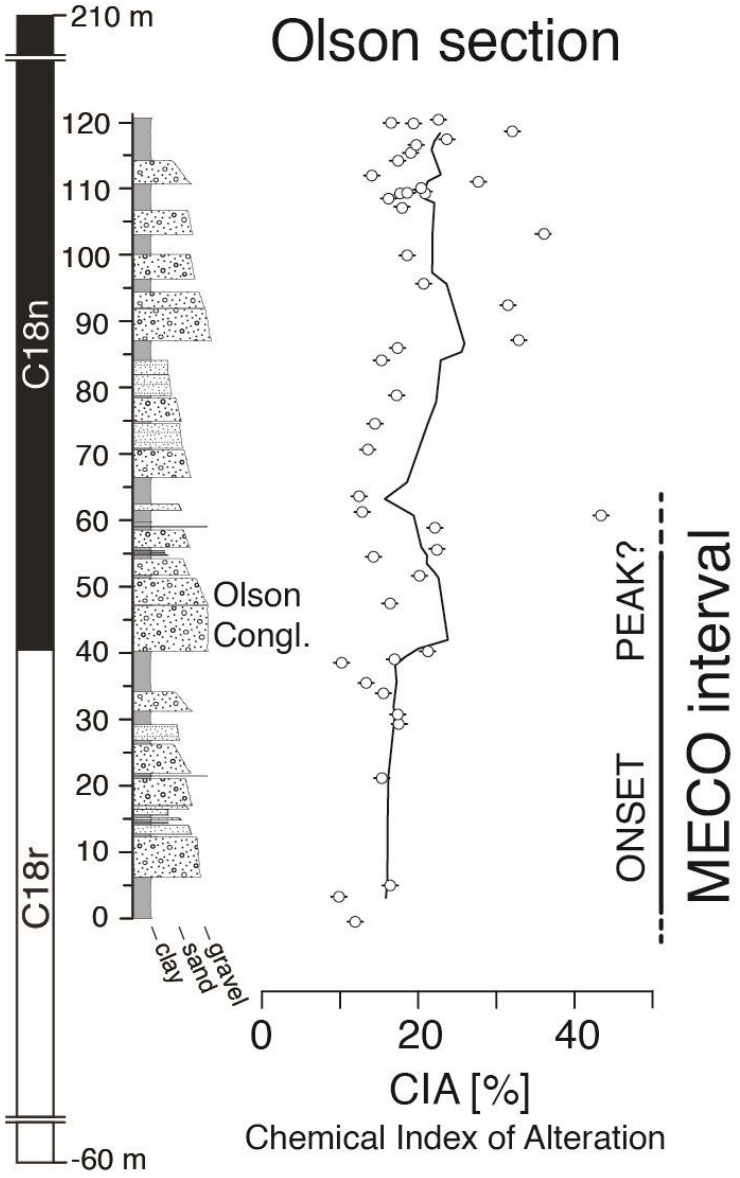

Figure 7. Chemical Index of Alteration (CIA) and associated standard error values from paleosols (white circles) displayed with a 7-point moving average to quantify chemical weathering in the Escanilla Fm at Olsón.”

Line 375 – 379: Modified Figure 8 and caption of Figure 8

“

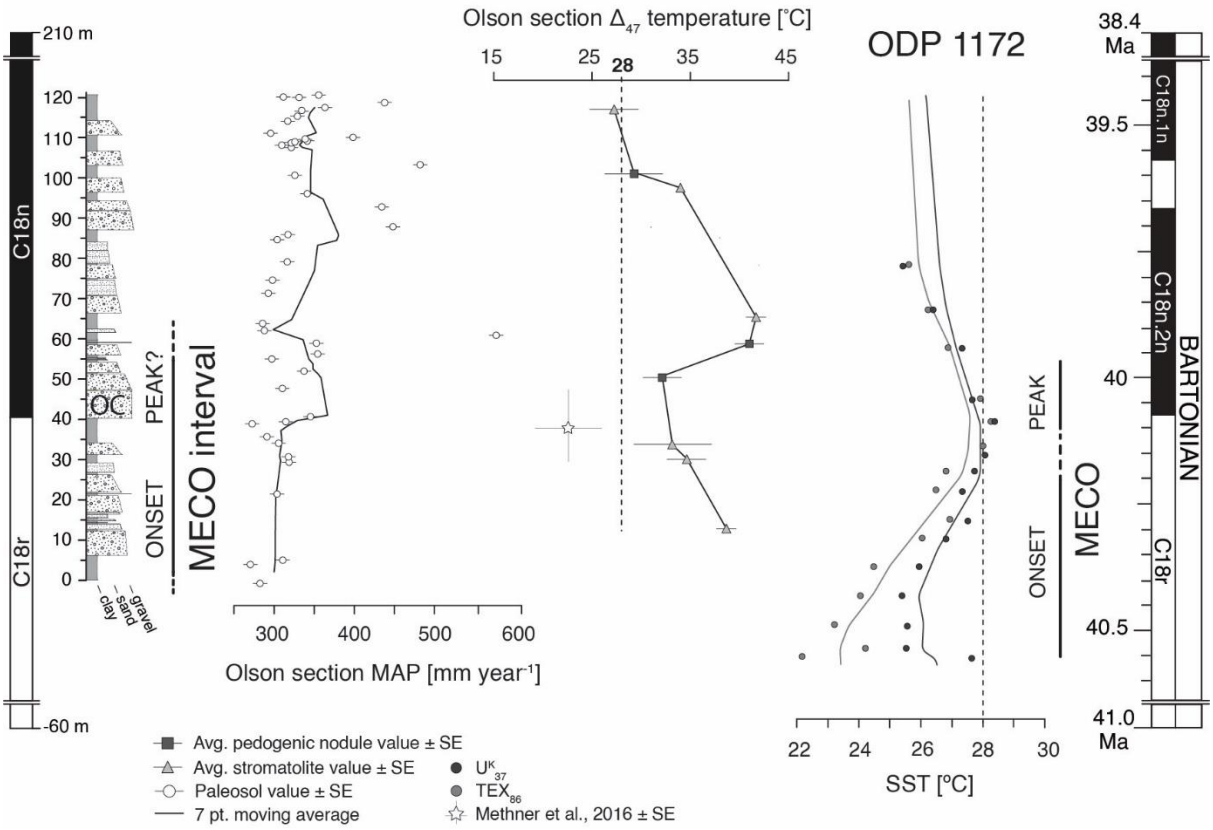

Figure 8. Mean annual precipitation (MAP) values (white circles) and the associated standard error from the Olsón section are presented using a 7-point moving average, followed by mean clumped isotope (Δ_{47}) temperatures and the standard error from replicate measurements of stromatolites (grey triangles) and pedogenic nodules (black squares). We compare our terrestrial temperature estimates to sea surface temperature proxies TEX_{86} and U^{K}_{37} (Bijl et al., 2010).”

Line 444 – 448: Modified Figure 9 and caption of Figure 9

“

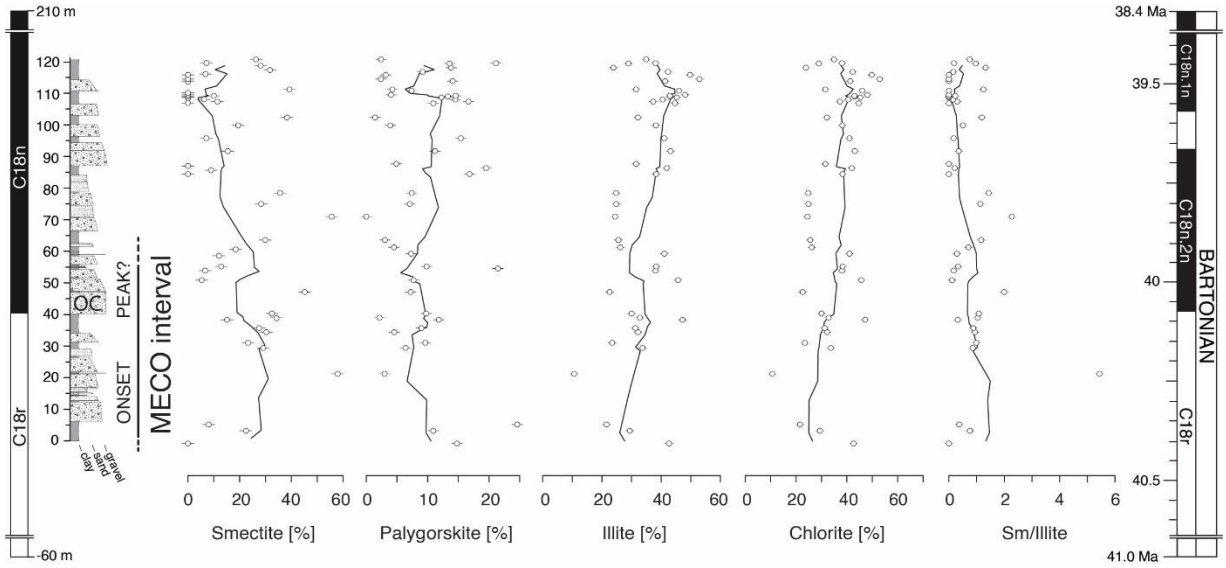

Figure 9. Identified clay mineral assemblages (smectite, palygorskite, illite, chlorite) and smectite/illite ratios are presented with respective standard error values and a 7-point moving average (black line) across the studied Escanilla Formation at Olsón. These minerals constitute up to 98% of the total clay mineralogy and suggest the presence of an arid to semi-arid climate under weak chemical weathering conditions during the MECO in the southern Pyrenees, Spain.”

3) Carbonate diagenesis

Carbonate minerals are extremely susceptible to diagenetic alteration. The authors interpreted the measured compositions as primary signals but did not provide evidence for the lack of diagenesis. And the possibility of diagenesis is not mentioned/discussed until the very end of the manuscript.

We agree that carbonate minerals and extremely susceptible to diagenetic alteration and can modify the primary signature and assessing the degree of diagenetic alteration is of prime importance before interpreting environmental conditions. To address this issue, we have added a new part titled “primary versus diagenetic signals” in the results and discussion section.

<u>Changes performed in MS:</u>

Line 305 – 323: Added

“4.3 Primary versus diagenetic signals

Carbon and oxygen isotope composition of bulk paleosol carbonates may be affected by the diagenetic alteration of mineral phases. It is therefore important to evaluate the potential diagenetic overprint on primary geochemical signatures (e.g., Marshall, 1992).

The degree of alteration was assessed through the relationship between $\delta^{13}C_{org}$ and $\delta^{13}C_{carb}$, and between $\delta^{18}O_{carb}$ and $\delta^{13}C_{carb}$ values. Pearson correlation coefficient, $r < 0.6$, indicates a statistically non-significant relationship and indicates that a diagenetic overprint on the primary signal can be excluded (e.g., Fio et al., 2010). In both correlation plots (Figure 6), no statistically significant correlation was found ($\delta^{13}C_{carb}$ vs $\delta^{13}C_{org}$: r = 0.21 (P = .16, N = 45), $\delta^{13}C_{carb}$ vs $\delta^{18}O_{carb}$: r = 0.05 (P = .74, N = 45)) indicating almost none or very minor diagenetic modification of the primary signal. Also, no correlation trend was observed between TOC and $\delta^{13}C_{org}$ (supplementary material; Figure S1).

Maximum Temperature (T_{max}) from rock eval analysis was used as a second approach to assess diagenetic alteration. T_{max} obtained in samples with high TOC (> 0.5 Wt. %) was < 440 °C which is the beginning of the oil window and indicates immature organic content (ca 60 °C, Espitalié et al., 1985).

As a third approach, paleosol samples (S9, S12, S17, S30) were analyzed using scanning electron microscopy (SEM). SEM images show presence of authigenic calcite (supplementary material, Figures S2 – S4), presence of authigenic clay minerals palygosrkite and smectite (supplementary material, Figures S5) and detrital illite and chlorite (supplementary material, Figures S6). Collectively, the three approaches suggest that the primary signal is largely preserved in the Escanilla Fm at Olsón."

Line 324: Added Figure 6

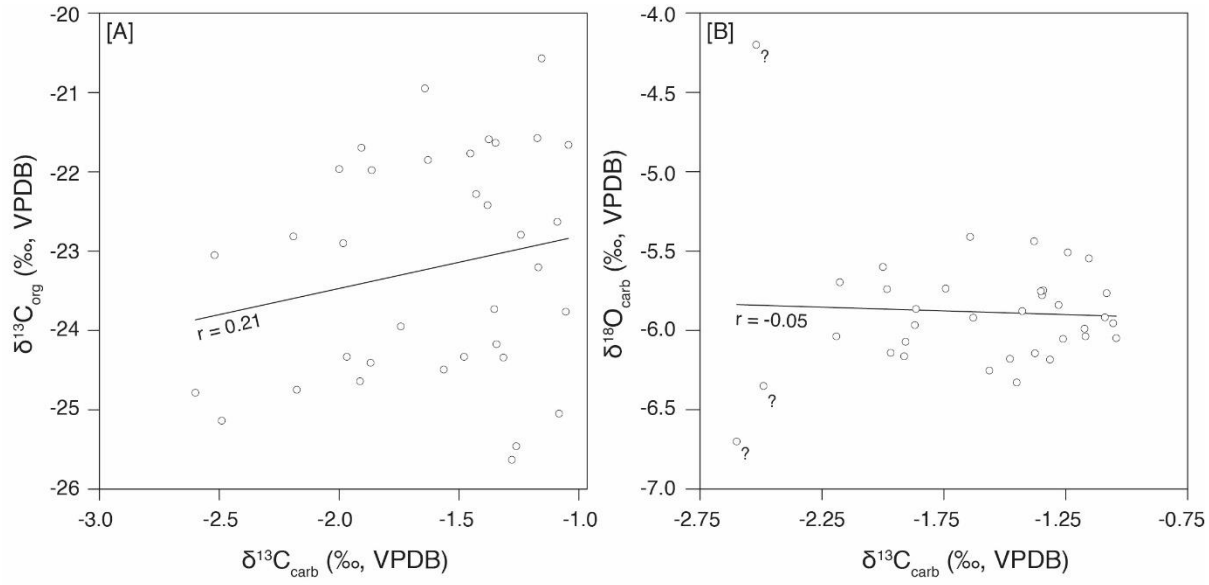

Line 325 – 326:

"Figure 6. (A) Scatter plot of paleosol $\delta^{13}C_{carb}$ vs $\delta^{13}C_{org}$ values (B) Scatter plot of paleosol $\delta^{13}C_{carb}$ vs $\delta^{18}O_{carb}$ values. For both plots, Pearson correlation coefficient (r) and regression line is shown."

4) CIA/chemical weathering/clays

The chemical index of alteration (CIA) can be modulated by other factors such as grain size (e.g. von Eynatten et al., 2012) and is not solely indicative of the degree of chemical weathering. And the characterization of lithology/source rock from which the sediments were derived from is important (but currently missing) for the interpretation of the measured CIA and clay mineralogy.

We agree that characterizing the lithology of the source rock is important for the interpretation of the measured CIA and clay mineralogy data. However, we would like to point out that the mentioned reference 'Von Eynatten et al., 2012' is based on sediment generation in a glacial setting where chemical processes are negligible. This is however not the case in our study. In fact, under global warming conditions such as the MECO or during previous hyperthermals such as the PETM, chemical weathering plays a very active role and hence CIA values are typically quite high (75 – 85%) during these intervals. Hence CIA values presented here are directly indicative of the extent of chemical weathering.

Changes performed in MS:

Line 59 – 73: Added new subsection 'The Escanilla sediment routing system' to describe how and from where sediments were sourced.

"2.1 The Escanilla sediment routing system

The Escanilla sediment routing system, situated in the Pyrenees, represents a well-preserved mid- to late Eocene-age (ca. 41 – 34 Ma) fluviatile succession. Catchment areas of the high Pyrenees were linked to the southern Pyrenean foreland Basin through the Sis and Gurb paleovalleys (Figure 1A) (Bentham et al., 1993; Labourdette & Jones 2007; Labourdette 2011; Michael et al., 2013). Extensive paleocurrent data suggests that these paleovalley systems predominantly derived sediments from the axial zone of the Pyrenees, converging in the Viacamp area (Figure 1A). From this point, sediments were carried downstream to the west through the Ainsa Basin (Vincent 2001; Whittaker et al., 2011; Parsons et al., 2012; Michael et al., 2013) into the shallow marine Jaca Basin (Peris Cabré et al., 2023) (Figure 1A).

The entire Escanilla sediment routing system has been meticulously documented within a comprehensive source-to-sink framework based on provenance tools, including clast lithologies (Mesozoic carbonates, Upper Carboniferous to Triassic clastic and igneous rocks, Hercynian granites, Paleozoic basement), heavy minerals, U–Pb geochronology of detrital zircons, apatite fission track analysis, paleocurrent analysis, magneto and biostratigraphy. Detailed explanation of this system can be found in the works of Michael et al. (2013, 2014b) and references therein."

Line 110: Added new subfigure (A) to Figure 1 to depict map of the Escanilla sediment routing system from source-to-sink.

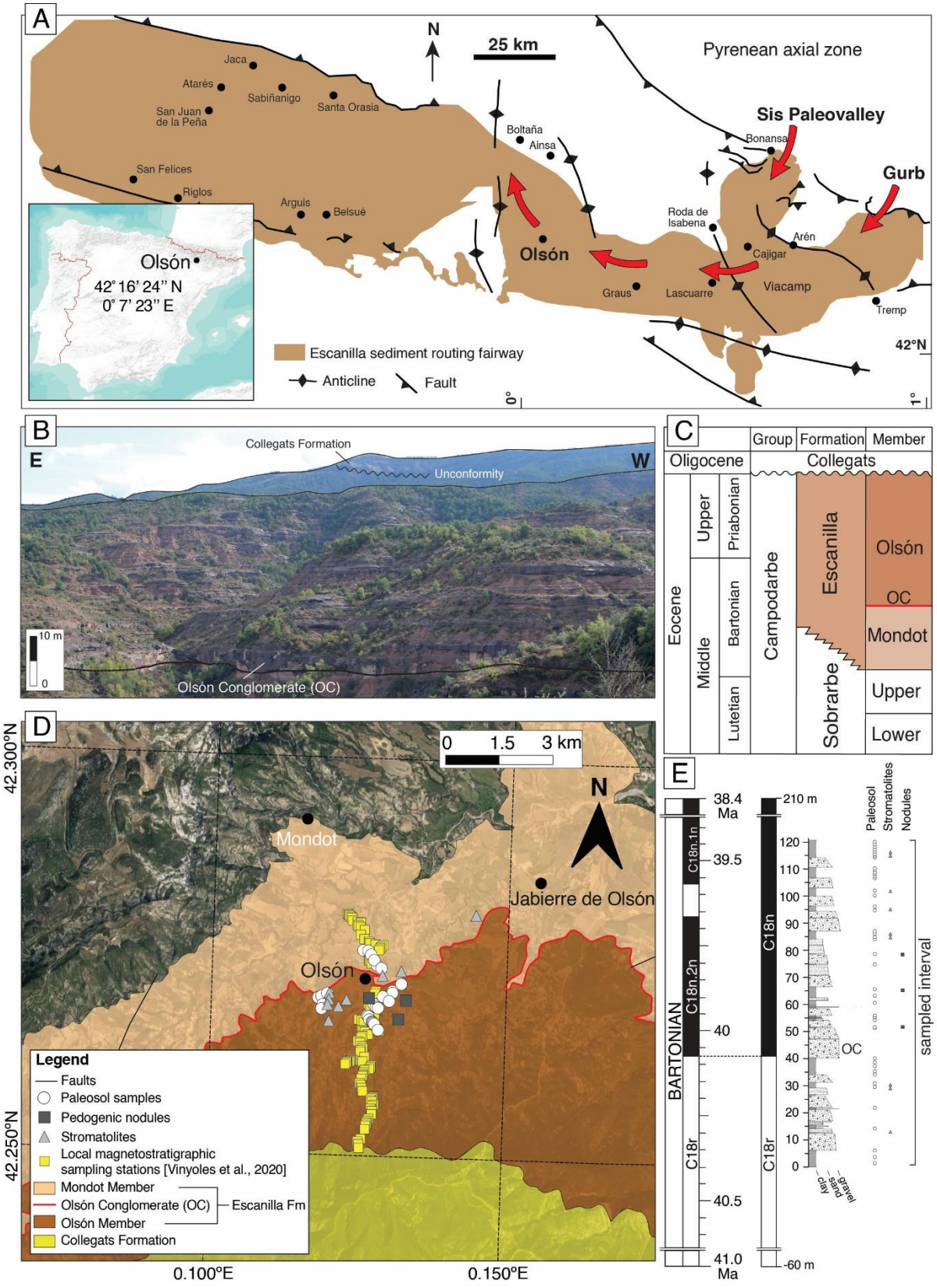

Line 111 – 120: Caption of Figure 1

"Figure 1 (A) Map of the Escanilla paleo-sediment routing system in the southern Pyrenees, Spain, also showing the main tectonic structures. Red arrows mark the water discharge and sediment transport direction of the Escanilla system away from the source regions of Sis and Gurb paleovalleys in the axial zone of the Pyrenees. Figure modified after Michael et al. (2014a). Also displayed is an inset map of Spain, indicating the study area near the village of Olsón. Map modified from Labourdette & Jones (2007). (B) Field image depicting the sampled Escanilla Fm. (C) Lithostratigraphic framework of the Escanilla Fm at Olsón consists of two main Members – the Mondot and the Olsón members with the Olsón Conglomerate (OC, red line) at the transition between the two Members. (D) Map showing the extent of the Escanilla Fm in northern Spain. (E) Sampled composite section, with position of each collected sample, of the Escanilla Fm together with the local magnetostratigraphic interpretation by Vinyoles et al. (2020) correlated to the Geomagnetic Polarity Time Scale (GPTS 2020) (Ogg, 2020). The thickest normal magnetozone C18n in the local magnetostratigraphic interpretation includes C18n.1n, C18n.1r, and C18n.2n."

Line 421 – 443: Modified discussion of clay mineralogy data

"Clay mineral assemblages in paleosols are also important paleoclimatic indicators and reflect detrital mineral input, composition of the source area lithology, type of weathering of the source rocks, to provide integrated records of the overall climate (Singer 1984; Franke & Ehrmann 2010; Rego et al., 2018).

Smectite, palygorskite, illite, and chlorite form up to 98 % of the identified mineral assemblages in the studied section (Figure 9). Smectite, commonly derived from alteration of volcanic rocks, forms under seasonal rainfall conditions with a pronounced dry season (e.g., Singer, 1984; Tabor et al., 2014) and constitutes on average 17 % of the total identified clay mineral assemblage while individual values reach up to 58 %. Palygorskite, an authigenic mineral (supplementary material, Figure S5), is indicative of an arid to semi-arid environment where evapotranspiration exceeds precipitation (e.g., Birkeland, 1984; Singer, 2002; Meunier, 2005), and constitutes up to 25 % (average of 10 %) of the total clay mineral assemblage. Illite content is between 11 and 53 % (average of 36 %), while chlorite content is between 7 to 64 % (average of 35 %) in the analyzed paleosols. High amounts of illite and chlorite, both detrital minerals (supplementary material, Figure S6), are typically found in sediments formed by physical erosion of low-grade metamorphic rocks and are thus indicative of weak, incipient chemical weathering (Tabor et al., 2014; Rego et al., 2018), and support our calculated CIA values. Except for palygorskite, clay mineral variations can be inferred to reflect weathering conditions in the source area of the Escanilla sediment routing system.

Increase in authigenic palygorskite content above the OC indicates environmental conditions on land became drier which is in agreement with previous studies showing an increase in aridification following the MECO interval in NW China (Bosboom et al., 2014)

and in the Neo-Tethys (Baskil section, eastern Turkey; Rego et al., 2018). This is also in agreement with our decreasing smectite/illite ratios above the OC (Figure 9) and is consistent with values reported by Rego et al. (2018). Overall, interpretation of clay mineral assemblages corroborates well with environmental conditions deduced from organic carbon stable isotopes data, weathering indices and mean annual precipitation."

Line by line:

Line 168-169: What defines an excursion? There may be a slight decrease in the seven-point average d13C_org values between 30-50m, but the absolute magnitude of change in d13C_org appear to be the largest between ~80m and 110m – what makes the signal between 30-50m an "excursion" rather than natural variability? Also, the individual d13C_org values during the MECO period appears to be more variable than other part of the section, is this expected?

An excursion can be defined as either a positive or negative shift in values from the average background values. In our case, we observe a negative excursion in d13C_org values of 3 ‰ between 30 – 50 m. Above and below this interval, values are relatively constant around -21.5 ‰ and hence the negative excursion stands out. The observed negative shift is also sudden compared to the background values until 90 m. Above 90 m, we agree that a gradual decrease in values, although highly variable exists.

<u>Changes performed in MS:</u>

Line 222 – 236: Modified discussion of d13C_org values

"TOC content in paleosol samples varies from 0.01 ± 0.01 to 0.57 ± 0.01 Wt. % with an average value of 0.07 ± 0.01 Wt. % (N = 45) (Figure 3). Low TOC may be indicative of low primary productivity, in this case 'vegetation' including grasses and higher plants, and (cyno)bacteria or low preservation of organic matter due to an oxidizing (oxygenated) environment (Tyson, 1995).

The $\delta^{13}C_{org}$ values of the paleosols have a range between -26.0 ± 0.2 and -20.4 ± 0.2 ‰ with an average value of -23.2 ± 0.2 ‰ (N = 45) (Figure 3). A negative CIE is marked by a 3 ‰ shift from the base of the section (from 0 to 30 m), where the onset begins, followed by a plateau of low values (30 to 50 m) that gradually return to higher values 60 m upwards. This negative CIE is most likely coeval to the 0.5 ‰ negative excursion observed in the benthic foraminifera $\delta^{13}C_{cib}$ values from ODP sites 738 (Bohaty et al., 2009) (Figure 3), indicating a general agreement in the change of $\delta^{13}C$ values, even though absolute differences in the magnitude of excursions exist.

A similar large magnitude negative CIE was previously identified for the PETM within the intermontane Piceance Creek Basin of western Colorado (USA), where a negative CIE of about 3 ‰ was reported (Foreman et al., 2012). The $\delta^{13}C_{org}$ record from the Middle Eocene Alano di Piave section deposited in the marginal Tethys Ocean recorded a negative

CIE of about 1 ‰ (Spofforth et al., 2010) while the coeval shallow water Sealza section from Italy recorded a negative CIE of 2 ‰ (Gandolfi et al., 2023).”

Line 174-175: Statistical analyses are needed to show robust correlation between the two records, visual similarity is not a very strong argument.

We agree that statistical analyses are needed to show robust correlation between two records. However, in this case, since d13C_org and d13C_cib data are two different datasets whose range does not overlap. As a result, comparing the magnitude of excursion between the two records is the most appropriate method to test for similarity. However, to address this, we have included statistical tests where appropriate.

Changes performed in MS:

Line 309 – 315: Added

“The degree of alteration was assessed through the relationship between $\delta^{13}C_{org}$ and $\delta^{13}C_{carb}$, and between $\delta^{18}O_{carb}$ and $\delta^{13}C_{carb}$ values. Pearson correlation coefficient, $r < 0.6$, indicates a statistically non-significant relationship and indicates that a diagenetic overprint on the primary signal can be excluded (e.g., Fio et al., 2010). In both correlation plots (Figure 6), no statistically significant correlation was found ($\delta^{13}C_{carb}$ vs $\delta^{13}C_{org}$: r = 0.21 (P = .16, N = 45), $\delta^{13}C_{carb}$ vs $\delta^{18}O_{carb}$: r = 0.05 (P = .74, N = 45)) indicating almost none or very minor diagenetic modification of the primary signal. Also, no correlation trend was observed between TOC and $\delta^{13}C_{org}$ (supplementary material; Figure S1).”

Line 179: What’s the reason to use a 7-point moving average (as opposed to 3-point or no smoothing at all)?

Selecting the window size (number of samples over which a simple moving average is calculated) to smooth a time series data depends on several factors such as the total sample size and the level of detail required. A larger window size means more smoothing, but also more loss of detail while a smaller window size means less smoothing but also more noise and variability. There is no one size fits all approach applicable when it comes to deciding the appropriate window size. For our dataset, we found the 7-point moving average the most appropriate.

Changes performed in MS: None

Line 186: What are the “several factors”? d13C values cannot be interpreted only in terms of MAP if other factors are not constrained.

Changes performed in MS:

Line 244 – 245: Added

"This wide range in $\delta^{13}C$ values of plants is dependent on several factors such as temperature, altitude, latitude, and MAP (Schulze et al., 1996; Kohn, 2010)."

Line 193-194: why does the lack of closed canopy forest + dry conditions = sparse vegetation? Maybe provide a more detailed explanation.

Changes performed in MS:

Line 222 – 225: Added

"TOC content in paleosol samples varies from 0.01 ± 0.01 to 0.57 ± 0.01 Wt. % with an average value of 0.07 ± 0.01 Wt. % (N = 45) (Figure 3). Low TOC may be indicative of low primary productivity, in this case 'vegetation' including grasses and higher plants, and (cyno)bacteria or low preservation of organic matter due to an oxidizing (oxygenated) environment (Tyson, 1995)."

Line 250 – 253: Added

"A significant proportion of measured values have relatively high $\delta^{13}C$ values (> -23 ‰) that are characteristic of dry environments with MAP < 500 mm yr^{-1} (Kohn, 2010). Low primary productivity and low organic matter preservation complemented by elevated $\delta^{13}C_{org}$ values likely indicates sparse vegetation in a dry and arid ecosystem."

Line 220-221: what does "a more sensitive proxy for the MECO" mean and what are the implications? The absolute change of d13C maybe larger in the organic carbon isotope record, but the background d13C_org data is also more variable.

This specific sentence has been omitted in the revised version. Considering the diagenetic alteration of paleosol bulk carbonates and uncertainty involved in obtained trends, we have modified the text accordingly and only presented the obtained data.

Changes performed in MS:

Line 269 – 281:

"The $d^{13}C_{carb}$ values in paleosol bulk carbonates have a range of -2.6 ± 0.01 to -1.0 ± 0.01 ‰ with an average of -1.6 ± 0.01 ‰ (N = 45) (Figure 4). A transient decrease in $\delta^{13}C_{carb}$ values is observed at 40 m where a negative CIE of about 1.0 ‰ magnitude is considered to represent the MECO negative CIE in the Escanilla Fm, followed by an increase in $\delta^{13}C_{carb}$ values to -1.5 ‰ towards the top of the section (Figure 4). These values are most likely synchronous to the negative CIE recorded in paleosol organic matter.

$\delta^{13}C_{carb}$ values in stromatolites range from -3.9 ± 0.1 to -1.3 ± 0.1 ‰ with an average value of -2.5 ± 0.1 ‰ (N = 63, 5 to 9 replicate measurements from 9 sample horizons), while $\delta^{13}C_{carb}$ values in pedogenic nodules range from -4.9 ± 0.3 ‰ to -1.1 ± 0.3 ‰ with an average value of -3.2 ± 0.3 ‰ (N = 29, 9 to 10 replicate measurements from 3 sample horizons). Since sample size is limited stratigraphically, it does not permit a direct evaluation of the isotopic signal relative to the MECO. However, $\delta^{13}C_{carb}$ values from stromatolites and pedogenic nodules show a consistent 1 to 2 ‰ negative offset when compared to values from paleosol bulk carbonates, which is possibly due to the presence of detrital Mesozoic carbonates ($\delta^{13}C_{carb}$ = 0 ‰; Zamarreno et al., 1997) in the bulk sediments from the source area."

Line 229-232: where are the "normal paleosol values" from? Are stromatolites and pedogenic nodules effectively the same endmember? They form via different mechanisms and intuitively they may express different fractionation – references/evidence that support they can be considered the same endmember would be helpful. What's the uncertainty of the estimated fraction with pedogenic origin?

We have removed this part from the main text since we now have a part evaluating primary versus diagenetic signal in the isotope data. We also recognize that pedogenic nodules and stromatolites form under different mechanisms and cannot be considered the same end-members. We have therefore presented stromatolites and pedogenic nodule data separately and the corresponding figures displaying their data have different symbols.

<u>Changes performed in MS:</u>

Line 269 – 281:

"The $d^{13}C_{carb}$ values in paleosol bulk carbonates have a range of -2.6 ± 0.01 to -1.0 ± 0.01 ‰ with an average of -1.6 ± 0.01 ‰ (N = 45) (Figure 4). A transient decrease in $\delta^{13}C_{carb}$ values is observed at 40 m where a negative CIE of about 1.0 ‰ magnitude is considered to represent the MECO negative CIE in the Escanilla Fm, followed by an increase in $\delta^{13}C_{carb}$ values to -1.5 ‰ towards the top of the section (Figure 4). These values are most likely synchronous to the negative CIE recorded in paleosol organic matter.

$\delta^{13}C_{carb}$ values in stromatolites range from -3.9 ± 0.1 to -1.3 ± 0.1 ‰ with an average value of -2.5 ± 0.1 ‰ (N = 63, 5 to 9 replicate measurements from 9 sample horizons), while $\delta^{13}C_{carb}$ values in pedogenic nodules range from -4.9 ± 0.3 ‰ to -1.1 ± 0.3 ‰ with an average value of -3.2 ± 0.3 ‰ (N = 29, 9 to 10 replicate measurements from 3 sample horizons). Since sample size is limited stratigraphically, it does not permit a direct evaluation of the isotopic signal relative to the MECO. However, $\delta^{13}C_{carb}$ values from stromatolites and pedogenic nodules show a consistent 1 to 2 ‰ negative offset when compared to values from paleosol bulk carbonates, which is possibly due to the presence of detrital Mesozoic carbonates ($\delta^{13}C_{carb}$ = 0 ‰; Zamarreno et al., 1997) in the bulk sediments from the source area."

Line 287 – 295:

"The $\delta^{18}O_{carb}$ values in paleosol bulk carbonates have a range between -6.7 ± 0.1 and -4.2 ± 0.1 ‰ with an average of -5.8 ± 0.1 ‰ (N = 45) (Figure 5). A positive OIE of ca 0.5 ‰ magnitude at 40 to 60 m, suggests an increase in freshwater ^{18}O content and perhaps represents peak MECO conditions in the Escanilla Fm. Peak warming would correspond to the OC where highest discharge and flux estimates have been predicted by Sharma et al. (2023). Following the positive OIE, $\delta^{18}O_{carb}$ values decline and return to relatively stable values of around -6.0 ‰, 60 m onwards until the top of the Olsón section and may represent the post-MECO cooling phase (Figure 5).

$\delta^{18}O_{carb}$ values in stromatolites range from -8.1 ± 0.1 to -4.7 ± 0.1 ‰ with an average value of -7.1 ± 0.1 ‰ (N = 63), while $\delta^{18}O_{carb}$ values in pedogenic nodules range from -7.6 ± 0.1 ‰ to -6.5 ± 0.1 ‰ with an average value of -6.9 ± 0.1 ‰ (N = 29); and crudely match the $\delta^{18}O$-trend in paleosol bulk carbonates (Figure 5)."

Line 301 – 307:

"In summary, irrespective of the presence of authigenic and detrital carbonates in paleosol samples, the negative CIE in paleosol organic matter suggests that the MECO can be regionally recognized in the Escanilla Fm. Stable isotope data from the Escanilla Fm at Olsón is also compatible with climate perturbations through excursions similar to the isotope excursions in the marine records, even though there are differences in the magnitude of excursions. These excursions have also been identified downstream in the time-equivalent marine sediments in the Jaca Basin, Spain (Peris Cabré et al., 2023) indicating the preservation of MECO climate perturbation signals in the source-to-sink Escanilla sediment routing system."

Line 287-288: what are the uncertainties with the MAP estimates? These appear to be very small variations, statistical analyses is needed to support your claims (i.e. there're actual changes).

Uncertainties associated with the MAP are presented in the form of standard error. A 20% increase in MAP is observed across the Olson Conglomerate (OC) with values outside the error margin. We therefore conclude that this increase in MAP most likely corresponds to peak MECO conditions.

Changes performed in MS:

Line 358 – 370: Modified

"MAP values in the Olsón section range from 270 ± 10 to 570 ± 10 mm year^{-1} with an average of 330 ± 10 mm year^{-1}. Values stay constant at 300 ± 10 mm year^{-1} until 40 m followed by a 20 % increase in precipitation, up to 370 ± 10 mm year^{-1}, which most likely corresponds to the OC (peak MECO conditions). Above the OC, MAP values return to an average value of 340 ± 10 mm year^{-1} until the top of the section (Figure 8). Overall, these values predict arid to semi-arid climate in this area of the southern Pyrenees during the Middle Eocene and are coherent with the high $\delta^{13}C_{org}$ values (water-stressed environments), low CIA and CIW values (diminished chemical weathering) in our section. At Igualada in the Ebro Basin, 200 km away from Olsón, palynological, pollen taxa and floral diversity studies suggest warm climate and humid vegetation, with preservation of mangrove swamp vegetation along the coast (Cavagnetto and Anadón 1996; Haseldonckx, 1972). The absence of humid climate in Olsón could be due to its location being higher in elevation and away from the coastline as compared to Igualada. Such regional differences in climate could also be the result of a climate transition phase during the Middle Eocene, oscillating from a warm tropical Early Eocene to a cold and arid Early Oligocene, expressed differently in different regions and at possibly different sampled intervals."

Line 299-310: a summary table with information (e.g. location, age, citation) of all the other records compared here would be helpful.

We agree that a summary table would be helpful, however all supporting documentation is available as supplementary material files accompanying this manuscript.

Changes performed in MS: None.

Line 307-310: I didn't fully follow the argument here. Why high Ca content results in underestimation of precipitation?

We have modified the text accordingly to avoid any confusion.

Changes performed in MS:

Line 371 – 378:

"MAP estimates based on well-dated megafloras from the Weisselster and Lausitz Basins (both in northeast Germany), consisting of shallow marine and continental deposits, are in the range of 1100 to 1400 mm year^{-1} (Mosbrugger et al., 2005). Other proxy data from southern France indicate a MAP less than 500 mm year^{-1} in the Bartonian (Kocsis et al., 2014), and is similar to our calculation from Spain. In conclusion, the values reported here should be regarded as being representative of a local signal, most likely influenced by rainshadow effects imposed by the Pyrenean topography at that time, which rose to 2000 meters between 49 and 41 Ma (Huyghe et al., 2012), thus possibly inducing orographic effects as observed in the modern situation (Vacherat et al., 2017; Huyghe et al., 2018)."

Line 333-334: if the samples are powdered, how come there's still inhomogeneity?

We have corrected the text.

Changes performed in MS:

Line 293 – 295:

"$d^{18}O_{carb}$ values in stromatolites range from -8.1 ± 0.1 to -4.7 ± 0.1 ‰ with an average value of -7.1 ± 0.1 ‰ (N = 63), while $d^{18}O_{carb}$ values in pedogenic nodules range from -7.6 ± 0.1 ‰ to -6.5 ± 0.1 ‰ with an average value of -6.9 ± 0.1 ‰ (N = 29); and crudely match the d^{18}O-trend in paleosol bulk carbonates (Figure 5)."

Line 341: how uncertain is this 400-kyr lag?

We have omitted referring to the 400-kyr lag in temperatures in the revised version.

Changes performed in MS: Modified

Line 403 – 412:

"Mean temperatures vary from 32.1 ± 1.8 °C to 38.6 ± 0.7 °C in the lower half of the section until 50 m followed by a peak mean temperature of 42 °C, just 25 m above the OC, without any observed change in lithology. Above 90 m until the top of the section, values return to an average value of 30 °C. Based on the available age constraints, our results suggest a potential lag between marine and terrestrial MECO climate signals. Our

results also suggest a land-sea temperature gradient of 5 to 10 °C when compared to sea surface temperature (SST) records from ODP site 1172 (Tasmania, Pacific; Bijl et al., 2010), and IODP sites U1408 and U1410 (northwest Atlantic Ocean; van der Ploeg et al., 2023) most likely indicating an amplifying effect due to continentality. Similar continental temperature sensitivity during the Middle Eocene has also been previously identified through clumped temperatures of pedogenic carbonates in the continental interiors of SW Montana, USA (Methner et al., 2016), Further research and sample analysis would however be required to investigate this further."

References:

Paola, C., Ganti, V., Mohrig, D., Runkel, A. C., & Straub, K. M. (2018). Time not our time: physical controls on the preservation and measurement of geologic time. Annual Review of Earth and Planetary Sciences, 46, 409-438.

von Eynatten, H., Tolosana-Delgado, R., & Karius, V. (2012). Sediment generation in modern glacial settings: Grain-size and source-rock control on sediment composition. Sedimentary Geology, 280, 80-92.